

# Network model of survival signaling in large granular lymphocyte leukemia

Ranran Zhang<sup>†</sup>, Mithun Vinod Shah<sup>†</sup>, Jun Yang<sup>†</sup>, Susan B. Nyland<sup>†</sup>, Xin Liu<sup>†</sup>, Jong K. Yun<sup>‡</sup>, Réka Albert<sup>§¶</sup>, and Thomas P. Loughran, Jr.<sup>†¶</sup>

<sup>†</sup>Penn State Hershey Cancer Institute and <sup>‡</sup>Department of Pharmacology, The Pennsylvania State University College of Medicine, Hershey, PA 17033; and <sup>§</sup>Department of Physics, The Pennsylvania State University, University Park, PA 16802

Edited by Wayne M. Yokoyama, Washington University School of Medicine, St. Louis, MO, and approved September 4, 2008 (received for review July 5, 2008)

T cell large granular lymphocyte (T-LGL) leukemia features a clonal expansion of antigen-primed, competent, cytotoxic T lymphocytes (CTL). To systematically understand signaling components that determine the survival of CTL in T-LGL leukemia, we constructed a T-LGL survival signaling network by integrating the signaling pathways involved in normal CTL activation and the known deregulations of survival signaling in leukemic T-LGL. This network was subsequently translated into a predictive, discrete, dynamic model. Our model suggests that the persistence of IL-15 and PDGF is sufficient to reproduce all known deregulations in leukemic T-LGL. This finding leads to the following predictions: (i) Inhibiting PDGF signaling induces apoptosis in leukemic T-LGL. (ii) Sphingosine kinase 1 and NF $\kappa$ B are essential for the long-term survival of CTL in T-LGL leukemia. (iii) NF $\kappa$ B functions downstream of PI3K and prevents apoptosis through maintaining the expression of myeloid cell leukemia sequence 1. (iv) T box expressed in T cells (T-bet) should be constitutively activated concurrently with NF $\kappa$ B activation to reproduce the leukemic T-LGL phenotype. We validated these predictions experimentally. Our study provides a model describing the signaling network involved in maintaining the long-term survival of competent CTL in humans. The model will be useful in identifying potential therapeutic targets for T-LGL leukemia and generating long-term competent CTL necessary for tumor and cancer vaccine development.

discrete dynamic model | nuclear factor kappa-B |  
signal transduction network | T box expressed in T cells |  
T cell large granular lymphocyte leukemia

Cytotoxic T lymphocyte (CTL) activation normally involves an initial expansion of antigen-specific CTL clones and their acquisition of cytotoxic activity. Subsequently, the activated CTL population undergoes activation-induced cell death (AICD), resulting in final stabilization of a small antigen-experienced CTL population (1). This process requires a delicate balance between proliferation, survival, and apoptosis. T cell large granular lymphocyte (T-LGL) leukemia is characterized by abnormal clonal expansion of antigen-primed mature CTL that successfully escaped AICD and remain long-term competent (2). Similar to normal activated CTL, leukemic T-LGL exhibit activation of multiple survival signaling pathways (3–5). However, unlike normal activated CTL, leukemic T-LGL are not sensitive to Fas-induced apoptosis (6), a process essential for AICD (7). Recent molecular profiling data suggest that normal CTL activation and AICD are uncoupled in leukemic T-LGL (8), providing a unique opportunity to decipher the key mediators of CTL activation and AICD in humans.

Network modeling has been increasingly used to better understand complex and interactive biological systems (9, 10). Experimentally obtained signaling pathway information can be translated into a graph (network) by representing proteins, transcripts, and small molecules as network nodes and denoting the interactions between nodes as edges (9). The direction of edges follows the direction of the mass or information flow, from

the upstream (source) node to the downstream (product or target) node. In addition, the edges are characterized by signs, where a positive sign indicates activation, and a negative sign indicates inhibition. Discrete dynamic modeling is widely used in modeling regulatory and signaling networks because of its straightforwardness, robustness, and compatibility with qualitative data (9–11). The simplest discrete models, called Boolean models, assume two possible states for each node in the network: ON (above threshold) and OFF (below threshold). The biological functions by which upstream regulators act on a downstream node can be readily translated into logical statements by using Boolean operators.

In this study, we aimed to systematically understand the long-term survival of competent CTL in T-LGL leukemia by constructing a T-LGL survival signaling network and a Boolean model of the network's dynamics. We found the constitutive presence of IL-15 and PDGF to be sufficient to reproduce all of the other signaling abnormalities. In addition, we studied the predicted key mediators of long-term CTL survival and their related signaling pathways.

## Results

**Constructing the T-LGL Survival Signaling Network.** We performed an extensive literature search and constructed the T-LGL survival signaling network (shown in Fig. 1) by adapting and simplifying a network describing the normal CTL activation–AICD process. The detailed method of network construction is described in [supporting information \(SI\) Text](#). The information used to construct the network, summarized by giving the source node, target node, two qualifiers of the relationship, and references, is given in [Table S1](#). The nomenclature of all of the nodes of the network before and after simplification is provided in [Tables S2 and S3](#). The T-LGL survival signaling network incorporates the most unique interactions through which all known deregulations in leukemic T-LGL are connected, in the context of normal CTL activation and AICD signaling. Proteins, mRNAs, and small molecules (such as lipids) were represented as nodes. “Cytoskeleton signaling”, “Proliferation” and “Apoptosis” were also included as nodes to summarize the biological effects of a group of components in the signaling pathways and serve as the

Author contributions: R.A. and T.P.L. designed research; R.Z., M.V.S., J.Y., and S.B.N. performed research; X.L. and J.K.Y. contributed new reagents/analytic tools; R.Z., M.V.S., J.Y., S.B.N., X.L., J.K.Y., R.A., and T.P.L. analyzed data; and R.Z., R.A., and T.P.L. wrote the paper.

The authors declare no conflict of interest.

This article is a PNAS Direct Submission.

<sup>¶</sup>To whom correspondence may be addressed at: Department of Physics, 122 Davey Laboratory, The Pennsylvania State University, University Park, PA 16802. E-mail: ralbert@phys.psu.edu.

<sup>¶</sup>To whom correspondence may be addressed at: Penn State Hershey Cancer Institute, 500 University Drive, Hershey, PA 17033. E-mail: tloughran@psu.edu.

This article contains supporting information online at [www.pnas.org/cgi/content/full/0806447105/DCSupplemental](http://www.pnas.org/cgi/content/full/0806447105/DCSupplemental).

© 2008 by The National Academy of Sciences of the USA

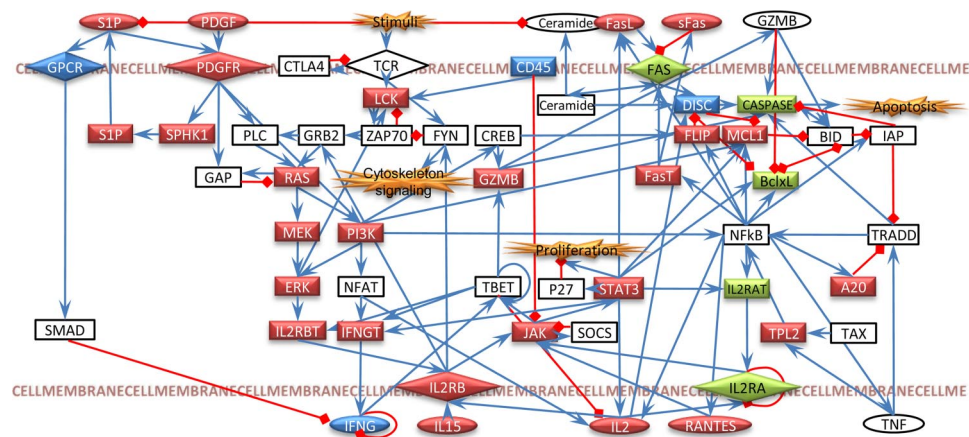


**Fig. 1.** The T-LGL survival signaling network. Node and edge color represents the current knowledge of the signaling abnormalities in T-LGL leukemia. Up-regulated or constitutively active nodes are in red, down-regulated or inhibited nodes are in green, nodes that have been suggested to be deregulated (either up-regulation or down-regulation) are in blue, and the states of white nodes are unknown or unchanged compared with normal. Blue edge indicates activation and red edge indicates inhibition. The shape of the nodes indicates the cellular location: rectangular indicates intracellular components, ellipse indicates extracellular components, and diamond indicates receptors. Conceptual nodes (Stimuli, Cytoskeleton signaling, Proliferation, and Apoptosis) are labeled orange. The full names of the node labels are provided in [Table S3](#).

indicators of cell fate. Because of the unknown etiology of T-LGL leukemia (2), we used “Stimuli” as a node to indicate antigen stimulation (12). This network contains 58 nodes and 123 edges. The biological description of the T-LGL survival signaling network is given in [SI Text](#).

**Translating the T-LGL Survival Signaling Network into a Predictive, Discrete, Dynamic Model.** To understand the dynamics of signaling abnormalities in T-LGL leukemia, we translated the T-LGL survival signaling network into a Boolean model. Each network node was described by one of two possible states: ON or OFF. The ON state means the production of a small molecule, the production and translation of a transcript, or the activation of a protein/process whereas the OFF state means the absence of a small molecule or transcript or the inhibition of a protein/process. The regulation of each component in the network was described by using the Boolean logical operators OR, AND, and NOT (see [Table S4](#)). OR represents the combined effect of independent upstream regulators on a downstream node whereas AND indicates the conditional dependency of upstream regulators to achieve a downstream effect. NOT represents the effect of inhibitory regulators and can be combined with activating regulations by using either OR or AND. The rules were derived from the regulatory relationships reflected in the network and from the literature. The detailed justification of the logical rules for all nodes in the network is provided in [SI Text](#). As in the biological system, there is a time lag between the state change of the regulators and the state change of the targets. The kinetics of signal propagation is rarely known from experiments. Thus, we used an asynchronous updating algorithm (10, 11) that samples differences in the speed of signal propagation. The detailed algorithm is described in [SI Text](#).

To reproduce how a population of cells responds to the same signal and to simulate cell-to-cell variability, we performed multiple simulations with the same initial conditions but different updating orders (i.e., different timing). The model was allowed to update for multiple rounds until the node Apoptosis became ON in all simulations (recapitulating the death of all CTL) or stabilized in the OFF state in a fraction of simulations (recapitulating the stabilization of the long-term surviving CTL population). The state of Stimuli was set to ON at the beginning of every simulation, recapitulating the activation of CTL by antigen. The states of the other nodes were set according to their

states in resting T cells, as described in the [SI Text](#). At the end of the simulation, if the state of a node stabilized at ON even though it was OFF at the beginning of the simulation, we consider it as constitutively active. If the state of a node stabilized at OFF even though it was in the ON state at the beginning of the simulation, or it was experimentally shown to be active after normal CTL activation, we consider it as down-regulated/inhibited. During simulations, the state of a node can be fixed to reproduce signaling perturbations.

#### Constitutive Presence of IL-15 and PDGF Is Predicted to Be Sufficient to Induce All of the Known Signaling Abnormalities in Leukemic T-LGL.

Zambello *et al.* (13) has demonstrated the presence of membrane-bound IL-15 on leukemic LGL, suggesting a role of IL-15 in the pathogenesis of this disease. In the course of studying constitutive cytokine production in LGL leukemia (14), we used a protein array as an experimental method. Using this array, we had found high levels of PDGF in LGL leukemia sera (unpublished observation). PDGF exists in the form of homodimers or heterodimers of two polypeptides: PDGF-A and PDGF-B (15). In the current study, we examined the level of PDGF-BB level in the sera of 22 T-LGL leukemia patients and 39 healthy donors and found that PDGF-BB was significantly higher in patient serum compared with normal ( $P < 0.005$ ) (Fig. 2A). We subsequently incorporated this deregulation into the network model.

To investigate signaling abnormalities underlying long-term survival of leukemic T-LGL, we first tested whether our model could reproduce the uncoupling of CTL activation and AICD by using all known deregulations (summarized in [Table S5](#)). We did not observe the activation of the node Apoptosis in any simulation. Second, we probed whether all of the deregulations have to be individually initiated or whether a subset of them can cause the others. The effect of a single signaling perturbation can be identified by keeping the state of the corresponding node according to its deregulation and tracking the states of other nodes until a stable (time-independent) state is obtained. IL-15, PDGF, and Stimuli are three nodes that have been suggested to be abnormal in T-LGL leukemia without known upstream regulators in the T-LGL survival-signaling network. To recapitulate the effect of their deregulations without masking the effect of the perturbation tested, the states of IL-15, PDGF, and Stimuli were randomly set at ON or OFF at every round of

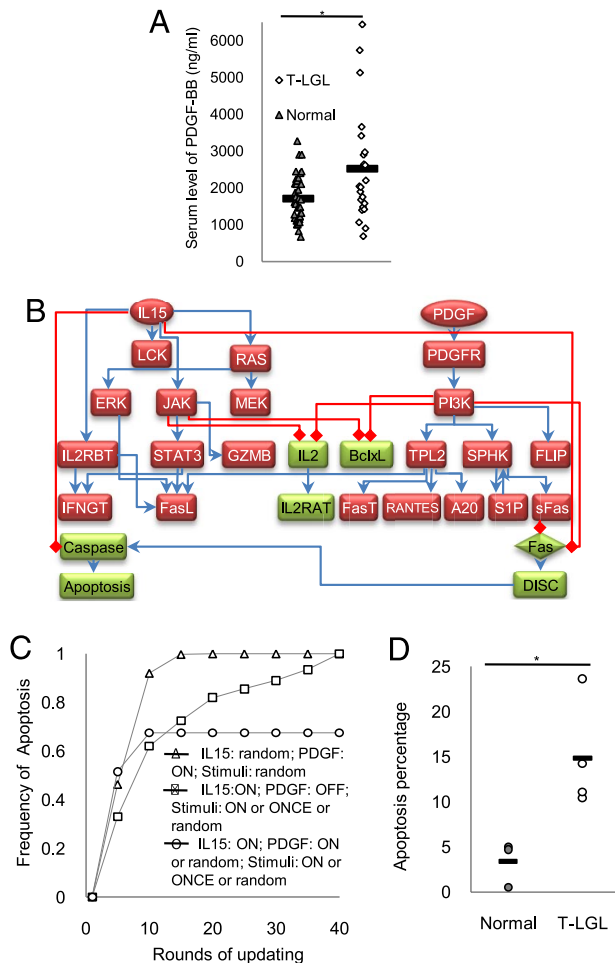


**Fig. 2.** The Boolean model of the T-LGL survival signaling network predicts that constitutive presence of IL-15, and PDGF is sufficient to induce all of the known deregulations in T-LGL leukemia. (A) PDGF-BB is elevated in T-LGL leukemia patient sera compared with normal. Serum level of PDGF-BB from 39 healthy donors (gray triangles) and 22 T-LGL leukemia patients (white diamonds) was assessed by using ELISA. The figure shows a 1.4-fold increase of mean serum level of PDGF-BB (black bar) in T-LGL leukemia patients compared with normal (\*,  $P < 0.005$ ). (B) Hierarchy among known signaling deregulations in T-LGL leukemia. Color code for nodes and edges is the same as in Fig. 1. (C) The effects of IL15, PDGF, and Stimuli on the frequency of apoptosis during simulation. Keeping PDGF ON does not prevent the onset of apoptosis (white triangles). While keeping IL-15 ON, keeping PDGF OFF from the first round of updating delays but cannot prevent the onset of apoptosis (white squares). Setting Stimuli ON at the beginning of the simulation and then keeping it OFF ("ONCE") does not alter the inhibition of apoptosis upon keeping IL-15 ON in the presence of PDGF (white circles). Results were obtained from 400 simulations of each initial condition. (D) 10  $\mu$ M AG 1296 specifically induced apoptosis in T-LGL leukemia PBMCs (white circles,  $n = 4$ ) after 24 h but not in normal PBMCs (gray circles,  $n = 3$ , \*,  $P < 0.03$ ). Each circle represents data from one patient or healthy donor. The markers (black bars) indicate the mean apoptosis percentage.

updating, i.e., in a random state, except when probing for the effect of their own deregulations.

Through this analysis, we discovered a hidden hierarchy among the known deregulations in leukemic T-LGL, with upstream deregulations as the potential cause of downstream deregulations. We present these regulatory relationships as a hierarchical network in Fig. 2B. Details of the hierarchy analysis are provided in *SI Text*. Surprisingly, we found that keeping the state of IL-15 at ON was sufficient to reproduce all known deregulations in leukemic T-LGL when setting a random state

for PDGF and Stimuli (Fig. S1). To understand the effect of PDGF and Stimuli individually upon the constant presence of IL-15, we probed all of the possible states of PDGF and Stimuli. We determined that the presence of PDGF is needed for the long-term survival of leukemic T-LGL. In contrast, the constitutive presence of Stimuli is not required after its initial activation (Fig. 2C). We concluded that based on the available signaling information regarding T cell activation and AICD, the minimal condition required for our model to reproduce all known signaling abnormalities in T-LGL leukemia (i.e., a T-LGL-like state) is IL-15 constantly ON, PDGF intermittently ON, and Stimuli ON in the initial condition.

To test the unexpected prediction that PDGF signaling, together with IL-15, maintains leukemic T-LGL survival, we inhibited PDGF receptor by using its specific inhibitor AG 1296. As shown in Fig. 2D, AG 1296 induced apoptosis specifically in T-LGL leukemia peripheral blood mononuclear cells (PBMCs) but not in normal PBMCs ( $n = 3-4$ ,  $P < 0.03$ ).

### Sphingosine kinase 1 (SPHK1) Is Important for the Survival of Leukemic T-LGL.

The next question we asked was: Can we identify the key mediators that determine the uncoupling of CTL activation and AICD in T-LGL leukemia? In our experimental system, the indication that a protein (small molecule or complex) is a key mediator in the finding that altering its amount or function can induce apoptosis in leukemic T-LGL. Accordingly, a corresponding network node is a key mediator if its state stabilizes once a T-LGL-like state is achieved, and altering its state increases the frequency of the ON state of Apoptosis. The detailed method to identify key mediators is provided in *SI Text*. As summarized in Table S6, experiments already suggested nine key mediators. We first tested whether our model could identify the corresponding nodes as key mediators. A rapid increase of apoptosis frequency was observed after resetting and maintaining the states of all of the known key mediators individually to their opposite states (from ON to OFF or from OFF to ON) after reproducing a T-LGL-like state. Examples of simulation results are provided in Fig. S2.

Based on this result, we systematically simulated the effect of individually altering the states of all nodes that stabilize when a T-LGL-like state is achieved. A list of these nodes is provided in Table S7. In addition to PDGF and its receptor, the model predicted seven additional key mediators: SPHK1, NF $\kappa$ B, S1P, SOCS, GAP, BID, and IL2RB, all exhibiting a similar dynamics of inducing apoptosis in the model. Fig. 3A shows the effect of inhibiting SPHK1 as an example. Recently, we found that the sphingolipid signaling is deregulated in leukemic LGL (8). Thus, we tested the effect of SPHK1 inhibition on leukemic T-LGL survival experimentally by using its chemical inhibitors, SPHK1 inhibitor-I and -II (SKI-I and SKI-II) (16, 17). As shown in Figs. 3B and C, both SKI-I and SKI-II significantly induced apoptosis in T-LGL leukemia PBMCs in a dose-dependent manner but not in normal PBMCs ( $n = 4-6$ ,  $P < 0.03$ ).

### NF $\kappa$ B Maintains the Survival of Leukemic T-LGL Through STAT3-Independent Regulation of myeloid cell leukemia sequence 1 (Mcl-1).

Our model predicts that NF $\kappa$ B is constitutively active and is a key mediator of the survival of leukemic T-LGL (Fig. 4A). Considering its importance in regulating T cell proliferation, cytotoxicity, and survival (18), we studied the activity and function of NF $\kappa$ B in T-LGL leukemia. As shown in Fig. 4B, nuclear extracts of normal PBMCs rarely exhibited NF $\kappa$ B activity as assessed by EMSA whereas NF $\kappa$ B activity was detected in most of the nuclear extracts of T-LGL leukemia PBMCs.

Next, we examined the effect of inhibiting NF $\kappa$ B by using its specific inhibitor BAY 11-7082 (19, 20). As shown in Fig. 4C, BAY 11-7082 inhibited the constitutive activity of NF $\kappa$ B in T-LGL leukemia PBMCs in a dose-dependent manner as as-

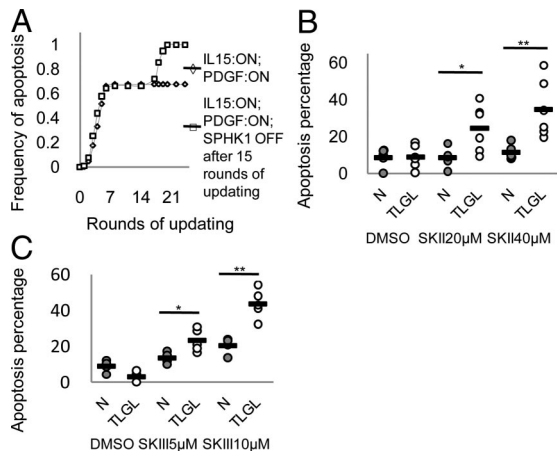


**Fig. 3.** SPHK1 is a key mediator for the survival of leukemic T-LGL. (A) The effect of SPHK1 inhibition on Apoptosis frequency in the model. The state of SPHK1 was reset to OFF after 15 rounds of updating (white squares), or left unchanged (white diamonds) after a T-LGL-like state was achieved. A rapid increase of apoptosis was observed after SPHK1 inhibition (200 simulations). (B) 20  $\mu$ M and 40  $\mu$ M SKI-I selectively induced apoptosis in T-LGL leukemia PBMCs ( $n = 6$ ) after 48 h but not in normal PBMCs ( $n = 5$ , \*,  $P < 0.03$  and \*\*,  $P < 0.01$ ). Each circle represents data from one patient or healthy donor. The markers (black bars) indicate the mean apoptosis percentage. (C) 5  $\mu$ M and 10  $\mu$ M SKI-II selectively induced apoptosis in T-LGL leukemia PBMCs after 48 h (white circles,  $n = 5$ ) but not in normal PBMCs (gray circles,  $n = 4$ , \*,  $P < 0.02$ , and \*\*,  $P < 0.001$ ). Each circle represents data from one patient or healthy donor. The markers (black bars) indicate the mean apoptosis percentage.

essed by EMSA. BAY 11–7082 (1  $\mu$ M) significantly induced apoptosis in T-LGL leukemia PBMCs but not in normal PBMCs ( $n = 6$ ,  $P < 0.009$ ) (Fig. 4D).

Based on the Boolean logical rule for NF $\kappa$ B (see Table S4),

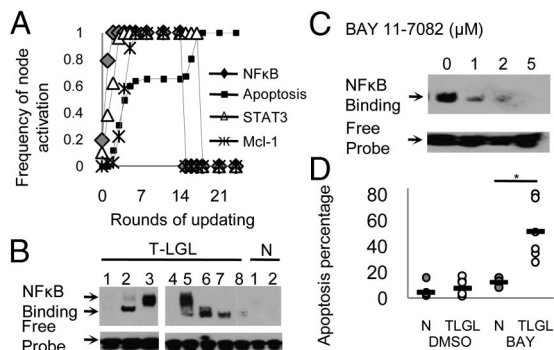


**Fig. 4.** NF $\kappa$ B is constitutively active in T-LGL leukemia and mediates survival of leukemic T-LGL. (A) Model prediction of the effects of NF $\kappa$ B inhibition (200 simulations). The state of NF $\kappa$ B was reset from ON to OFF after 15 rounds of updating, while keeping IL-15 and PDGF ON. Apoptosis (black squares) was rapidly induced after inhibiting NF $\kappa$ B (black diamonds). The induction of apoptosis was tightly coupled with the down-regulation of Mcl-1 (x). In contrast, the state of STAT3 (white triangles) remained unchanged until the simulation was terminated. (B) NF $\kappa$ B activity in nuclear extracts of PBMCs from healthy donors and T-LGL leukemia patients. EMSA results are representative of 16 healthy donors and 8 T-LGL leukemia patients tested. White space has been inserted to indicate realigned gel lanes. (C) BAY 11–7082 inhibits NF $\kappa$ B activity in T-LGL leukemia PBMCs. T-LGL leukemia PBMCs were treated with vehicle DMSO or 1  $\mu$ M, 2  $\mu$ M, or 5  $\mu$ M BAY 11–7082 for 3 h, and the activity of NF $\kappa$ B was assessed by EMSA. Result is representative of experiments in three patients. (D) Compared with normal PBMCs (black circles,  $n = 6$ ), 1  $\mu$ M BAY 11–7082 selectively induced apoptosis in T-LGL leukemia PBMCs (white circles,  $n = 6$ ) after 12h treatment (\*,  $P < 0.02$ ). Each circle represents data from one patient or healthy donor. The markers (black bars) indicate the mean of each sample group.

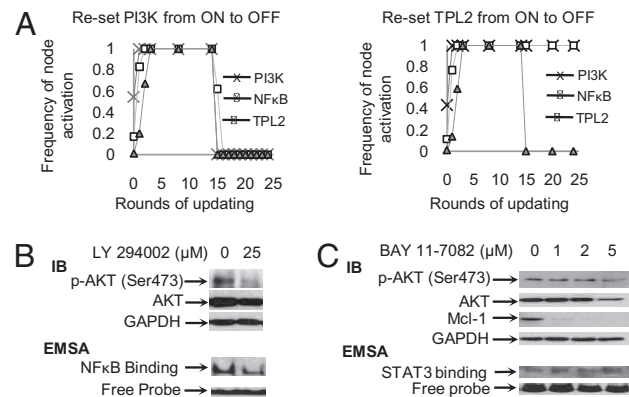


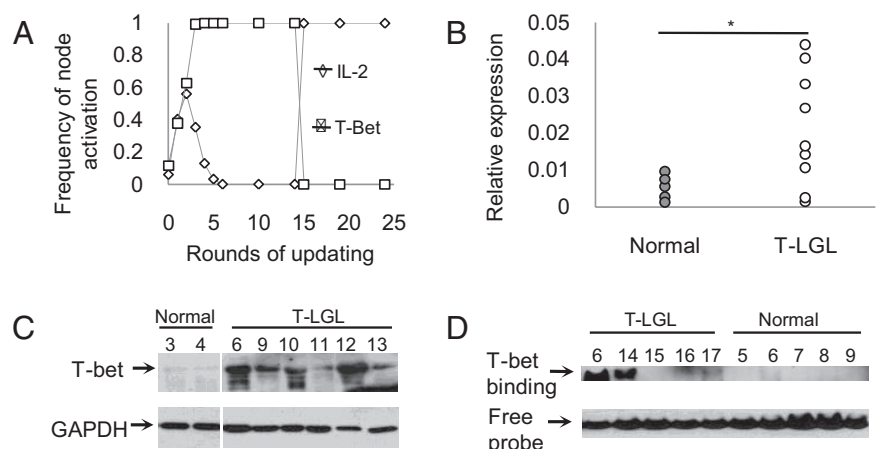
**Fig. 5.** NF $\kappa$ B-mediated survival pathway in T-LGL leukemia involves PI3K and Mcl-1. (A) Analysis of the potential cause(s) of the constitutive activation of NF $\kappa$ B. As in Table S4, the Boolean logical rule governing the state of NF $\kappa$ B is “NF $\kappa$ B\* = [(TPL2 or PI3K) or (FLIP and TRADD and IAP)] and not Apoptosis”. When a T-LGL-like state is achieved, the state of TRADD stabilizes at OFF (see Table S7). Thus, the node that activates NF $\kappa$ B can only be TPL2 or PI3K, which are known to be constitutively active in T-LGL leukemia (see Table S5). Rapid inhibition of NF $\kappa$ B (white squares) was observed after inhibiting PI3K (X) but not after inhibiting TPL2 (gray triangles) (200 simulations). (B) PI3K inhibition induced NF $\kappa$ B inhibition in T-LGL leukemia. T-LGL leukemia PBMCs were treated with vehicle DMSO or 25  $\mu$ M LY 294002 for 4 h. The amount of total and phospho-AKT was assessed by Western blot assay; NF $\kappa$ B activity was assessed by EMSA. Result is representative of experiments in three patients. (C) NF $\kappa$ B inhibition down-regulates Mcl-1 but does not influence STAT3 activity and the PI3K pathway. T-LGL leukemia PBMCs were treated with vehicle DMSO or 1  $\mu$ M, 2  $\mu$ M or 5  $\mu$ M BAY 11–7082 for 3 h, and the amount of Mcl-1, total- and phospho-AKT was assessed by Western blot assay. STAT3 activity was assessed by EMSA. Result is representative of experiments in three patients. GAPDH was used as a loading control for all of the Western blot assays.

it can be activated by PI3K or tumor progression locus 2 (TPL2)/cancer Osaka thyroid. During simulations, however, we noticed that the ON state of NF $\kappa$ B was only determined by the constitutive activity of PI3K because resetting the state of PI3K from ON to OFF was necessary and sufficient to induce the rapid inhibition of NF $\kappa$ B whereas altering the state of TPL2 did not affect NF $\kappa$ B activity (Fig. 5A). We then subjected the T-LGL leukemia PBMCs to PI3K specific inhibitor LY 294002 and tested the effect on NF $\kappa$ B activity. LY 294002 (25  $\mu$ M) significantly inhibited the activity of NF $\kappa$ B as assessed by EMSA (Fig. 5B) and induced apoptosis in T-LGL leukemia PBMCs (data not shown) as reported (4). BAY 11–7082 did not inhibit the activity (phosphorylation) of v-akt murine thymoma viral oncogene homolog (AKT), an immediate downstream target of PI3K in T-LGL leukemia PBMCs, as assessed by Western blot assay (Fig. 5C).

We found that for simulations in which we reset the state of NF $\kappa$ B from ON to OFF, the onset of apoptosis correlated tightly with the rapid down-regulation of Mcl-1 (Fig. 4A). It has been shown that STAT3 transcriptionally regulates Mcl-1 in leukemic T-LGL (3). Interestingly, our model predicted that the initial Mcl-1 down-regulation after NF $\kappa$ B inhibition was independent of STAT3 activity (Fig. 4A). Our experimental results confirmed this prediction. As shown in Fig. 5C, the amount of Mcl-1 after BAY 11–7082 treatment did indeed decrease correspondingly to the decreased NF $\kappa$ B activity whereas STAT3 activity remained unchanged after NF $\kappa$ B inhibition, as assessed by EMSA, even at the highest dose of BAY 11–7082.

**T box expressed in T cells (T-bet) Is Constitutively Active in Leukemic T-LGL.** It has been shown that leukemic T-LGL are incapable of producing IL-2 even upon *in vitro* stimulation (21). It has also been shown that NF $\kappa$ B promotes IL2 transcription (18). In our model, this apparent conflict can be resolved if T-bet is consti-

**Fig. 6.** T-bet is overexpressed and constitutively active in T-LGL leukemia PBMCs. (A) T-bet inhibits IL-2 expression when a T-LGL-like state is achieved. Based on the Boolean logical rule "IL2\* = (NFkB or STAT3 or NFAT) and not (TBet or Apoptosis)" (Table S4), T-bet is the only negative regulator of IL-2 expression when cells are still alive. Inhibiting T-bet (white squares) after 15 rounds of updating results in IL-2 (white diamonds) expression after achieving a T-LGL-like state (200 simulations). (B) T-LGL leukemia PBMCs (white squares,  $n = 10$ ) express 3.3-fold higher T-bet mRNA compared with normal (black circles,  $n = 5$ ,  $P < 0.02$ ) as assessed by real-time PCR. (C) T-bet protein expression in T-LGL leukemia and normal PBMCs. Western blot assay result is representative of samples from eight healthy donors and six T-LGL leukemia patients. White space has been inserted to indicate realigned gel lanes. (D) T-bet is constitutively active in T-LGL leukemia patients. Nuclear extract from PBMCs of five T-LGL leukemia patients and five healthy donors were tested for their T-bet activity by using EMSA. T-bet exhibited high activity in most T-LGL leukemia patients but not in normal.



tively active. As shown in Fig. 6A, when a T-LGL-like state was achieved, the state of T-bet stabilized at ON, and there was a rapid increase of IL-2 production when the state of T-bet was reset to OFF. In agreement with the model's prediction, T-bet was significantly elevated in T-LGL leukemia PBMCs compared with normal PBMCs at both mRNA and protein levels, as assessed by real-time PCR and Western blot assay (Figs. 6B and C). In addition, T-LGL leukemia PBMCs exhibited high T-bet activity as assessed by EMSA whereas the T-bet activity was almost undetectable in normal PBMCs (Fig. 6D).

## Discussion

The long-term survival of competent CTL in T-LGL leukemia offers a unique opportunity to reveal the key mediators of CTL activation and AICD in humans. In this study, we curated the signaling pathways involved in normal CTL activation, AICD, and the deregulations in leukemic T-LGL and compiled them into a T-LGL survival signaling network. By formulating a Boolean dynamic model of this network, we were able to identify the potential causes and key regulators of this abnormal survival.

Signaling pathways are complex and dynamic. However, experimental results are usually focused on limited interactions of the components in one pathway and neglecting the broader effects in the same or other pathways. Integrating existing pathway information to infer cross-talk among pathways is desirable, especially for studies in T-LGL leukemia where experimental data are limited. Using network theory as a tool, we identified the most unique interactions among known deregulated components in leukemic T-LGL in the context of CTL activation and AICD and summarized these signaling events in the form of a network. This served as an innovative platform to understand the abnormal CTL survival in T-LGL leukemia.

Multiple perturbations of signaling pathways in a disease can result from deregulation of only a subset of these pathways. However, identifying such a subset is difficult experimentally. In this study, we assessed this question in T-LGL leukemia by using a Boolean dynamic model. Through network simulations, we revealed the hierarchy among deregulated nodes in terms of determining other signaling abnormalities in leukemic T-LGL. The simultaneously constitutive presence of IL-15 and PDGF was shown to be sufficient to induce all known deregulations after initial T cell activation.

Leukemic T-LGL are suggested to be antigen-primed (12), long-term competent CTL (22), similar to terminally differentiated effector memory cells ( $T_{EMRA}$ ) (23). It is worth noting that IL-15 has been shown to be important for CTL activation and generation of long-lived CD8<sup>+</sup> memory cells (24, 25). Both the

CD8<sup>+</sup> cells in the *IL15* transgenic mice (26) and the *IL15* transduced primary human CD8<sup>+</sup> cells (27) indeed showed similar phenotypes as leukemic T-LGL. However, IL-15 alone cannot fully inhibit the onset of apoptosis in our model (Fig. 2C). Increased PDGF production occurs under inflammatory conditions (28), and it has been shown to exert an inhibitory effect toward CTL activation (29). We had found that LGL leukemia is characterized by production of proinflammatory cytokines (14). Here, we showed an increased level of PDGF in T-LGL patient sera. Our model and the following validation revealed that both pro- and anti-T cell activation signals are needed simultaneously to maintain the competency and survival of CTL in T-LGL leukemia. Our finding also suggests that provision of IL-15 and PDGF may be a strategy to generate long-lived CTL necessary for the development of virus and cancer vaccines.

Focusing on the effect of nodes on apoptosis in leukemic T-LGL, we revealed nodes that determine the uncoupling of CTL activation and AICD. We experimentally validated two predicted key mediators: SPHK1 and NF $\kappa$ B, the inhibition of which induces apoptosis in leukemic T-LGL. It is worth noting that although NF $\kappa$ B has been suggested to inhibit apoptosis in CTL (30), its function in maintaining long-term CTL survival remains elusive. We validated the prediction that NF $\kappa$ B is downstream of PI3K and prevents the onset of apoptosis in leukemic T-LGL through maintaining the expression of Mcl-1 independent of STAT3, another regulator of Mcl-1 in T-LGL leukemia (3).

The confirmation of the constitutive NF $\kappa$ B activation led to the validation of the constitutive T-bet activation in T-LGL leukemia predicted by our model. T-bet plays an important role in coupling the effector and memory CD8<sup>+</sup> T cell fate (31). It also inhibits the production of IL-2, which is known to be absent in leukemic T-LGL and in  $T_{EMRA}$  (23, 32). T-bet has been related to multiple autoimmune diseases in humans (33–36). T-LGL leukemia has important overlaps with autoimmune disorders, particularly rheumatoid arthritis (2). The overexpression and constitutive activity of T-bet in leukemic T-LGL may help to reveal the common pathogenesis between T-LGL leukemia and other autoimmune diseases.

With the exponential increase of signaling pathway information, it is becoming more difficult to determine pathway interactions in a particular experimental system. In this study, we used network analysis and Boolean modeling to investigate the signaling abnormalities in T-LGL leukemia. This systems biology approach was able to maximize the use of the available pathway information and to identify the key mediators of CTL survival, highlighting their importance as potential therapeutic targets for T-LGL leukemia

and offering insights into CTL manipulation. This study confirms the possibility of integrating normal and disease pathway information into a single model that is powerful enough to reproduce a clinically relevant complex process, useful for therapeutic purpose, yet is constructed with only qualitative information.

## Materials and Methods

**Patient Consent.** All patients met the clinical criteria of T-LGL (CD3+) leukemia with increased LGL counts and clonal T cell antigen receptor gene rearrangement. None of the patients received treatment for LGL leukemia. Informed consents were signed by all patients and age- and sex-matched healthy individuals allowed the use of their cells for these experiments. Buffy coats were obtained from Hershey Medical Center Blood Bank according to protocols observed by Milton S. Hershey Medical Center, Hershey, PA.

**Chemicals and Reagents.** All chemical reagents and LY 294002 were purchased from Sigma-Aldrich. AG 1296 and BAY 11-7082 was purchased from EMD Bioscience. LightShift Chemiluminescent EMSA Kit was purchased from Pierce Biotechnology. Human PDGF-BB Quantikine ELISA Kit was purchased from R&D systems. Annexin V-PE Apoptosis Detection Kit-I and TransFactor Extraction Kit were purchased from BD Biosciences. Biotinylated and nonbiotinylated DNA oligonucleotides were purchased from Integrated DNA Technology. Anti-Mcl-1 and anti-T-bet antibodies were purchased from Santa Cruz Biotechnology. Anti-AKT and anti-phospho-AKT (Ser-473) antibodies were purchased from Cell Signaling Technology. Anti-GAPDH antibody was purchased from Chemicon and Millipore. SPHK1 inhibitor I and II (SKI-I and SKI-II) were kindly provided by Dr. Jong K. Yun.

**ELISA.** Sera from 22 T-LGL patients and 39 age- and sex-matched healthy donors were prepared and analyzed according to manufacturer's instruction, as described (14).

**Cell Culture and Apoptosis Assay.** PBMCs were processed from blood samples of patients and Buffy coats of normal donors, and apoptosis assays were performed by using Annexin-V conjugated with phytoerythrocyanin (PE) and 7-amino-actinomycin-D staining as described (23). Each treatment was per-

formed and measured three times for one blood sample. Apoptosis was calculated by using the following formula:

$$\text{Percentage of specific apoptosis} = \frac{[(\text{Annexin-V-PE positive cells in treatment} - \text{Annexin-V-PE positive cells in control}) \times 100]}{(100 - \text{Annexin-V-PE positive cells in control})}$$

**Western Blot Assay.** Cell lysates were prepared, protein concentration was determined, and Western blot assay was performed as described (3).

**EMSA.** Nuclear and cytoplasmic extract from patient and normal PBMCs were prepared by using TransFactor Extraction Kit according to manufacturer's instructions. Probes for NF- $\kappa$ B (5'-GATCCGGCAGGGGAATCTCCCTCTC-3') (20), STAT3 (5'-CTTCATTTCCCGTAAATCCCTA) (3) and T-bet (5'-AAAACCTTGT-GAAAATACGTAATCCTCAG-3') (34) were biotinylated at 5'. Corresponding nonbiotinylated oligonucleotides were used as competition oligonucleotides. EMSA was performed by using the LightShift Chemiluminescent EMSA Kit according to manufacturer's instructions.

**Real-Time PCR.** Total RNA was processed as described (8). Primers specific for T-bet (forward: 5'-TGTGGTCCAAGTTAATCAGCA-3'; reverse: 5'-TGACAG-GAATGGGAACATCC-3') and glyceraldehyde-3-phosphate dehydrogenase (GAPDH, forward: 5'-GAGTCAACGGATTTGGTCGT-3'; reverse: 5'-TTGATTTG-GAGGGATCTCG-3') were used for real-time PCR and expression was quantified as described (8).

**Computational Methods.** Network simplification was performed with NET-SYNTHESIS, a signal transduction network inference and simplification tool (37, 38). The dynamic model was implemented in custom python code. Additional details regarding computational methods are given in the [S1 Text](#).

**ACKNOWLEDGMENTS.** We thank Nate Sheaffer and David Stanford for help with acquisition and analysis of flow cytometry data and Lynn Ruiz, Kendall Thomas, and Nancy Ruth Jarbada for help with acquiring patient samples and processing them. This work is supported by National Institutes of Health Grant R01 CA 94872. Boolean model development in R.A.'s group is supported by National Science Foundation Grant CCF-0643529.

1. Klebanoff CA, Gattinoni L, Restifo NP (2006) CD8+ T-cell memory in tumor immunology and immunotherapy. *Immunol Rev* 211:214–224.
2. Sokol L, Loughran TP, Jr (2006) Large granular lymphocyte leukemia. *Oncologist* 11:263–273.
3. Epling-Burnette PK, et al. (2001) Inhibition of STAT3 signaling leads to apoptosis of leukemic large granular lymphocytes and decreased Mcl-1 expression. *J Clin Invest* 107:351–362.
4. Schade AE, Powers JJ, Wlodarski MW, Maciejewski JP (2006) Phosphatidylinositol-3-phosphate kinase pathway activation protects leukemic large granular lymphocytes from undergoing homeostatic apoptosis. *Blood* 107:4834–4840.
5. Epling-Burnette PK, et al. (2004) ERK couples chronic survival of NK cells to constitutively activated Ras in lymphoproliferative disease of granular lymphocytes (LDGL). *Oncogene* 23:9220–9229.
6. Lamy T, Liu JH, Landowski TH, Dalton WS, Loughran TP, Jr (1998) Dysregulation of CD95/CD95 ligand-apoptotic pathway in CD3+ large granular lymphocyte leukemia. *Blood* 92:4771–4777.
7. Krueger A, Fas SC, Baumann S, Krammer PH (2003) The role of CD95 in the regulation of peripheral T-cell apoptosis. *Immunol Rev* 193:58–69.
8. Shah MV, et al. (2008) Molecular profiling of LGL leukemia reveals role of sphingolipid signaling in survival of cytotoxic lymphocytes. *Blood* 112:770–781.
9. Christensen C, Thakar J, Albert R (2007) Systems-level insights into cellular regulation: Inferring, analysing, and modelling intracellular networks. *IET Syst Biol* 1:61–77.
10. Li S, Assmann SM, Albert R (2006) Predicting essential components of signal transduction networks: A dynamic model of guard cell abscisic acid signaling. *PLoS Biol* 4:e312.
11. Chaves M, Albert R, Sontag ED (2005) Robustness and fragility of Boolean models for genetic regulatory networks. *J Theor Biol* 235(3):431–449.
12. Wlodarski MW, et al. (2005) Pathologic clonal cytotoxic T-cell responses: Nonrandom nature of the T-cell-receptor restriction in large granular lymphocyte leukemia. *Blood* 106:2769–2780.
13. Zambello R, et al. (1997) Interleukin-15 triggers the proliferation and cytotoxicity of granular lymphocytes in patients with lymphoproliferative disease of granular lymphocytes. *Blood* 89:201–211.
14. Kothapalli R, et al. (2005) Constitutive production of proinflammatory cytokines RANTES, MIP-1 $\beta$  and IL-18 characterizes LGL leukemia. *Int J Oncol* 26:529–535.
15. Helden C-H, Westermarck B (1999) Mechanism of action and in vivo role of platelet-derived growth factor. *Physiol Rev* 79:1283–1316.
16. French KJ, et al. (2003) Discovery and evaluation of inhibitors of human sphingosine kinase. *Cancer Res* 63:5962–5969.
17. French KJ, et al. (2006) Antitumor activity of sphingosine kinase inhibitors. *J Pharmacol Exp Ther* 318:596–603.
18. Hoffmann A, Baltimore D (2006) Circuitry of nuclear factor  $\kappa$ B signaling. *Immunol Rev* 210:171–186.
19. Pierce JW, et al. (1997) Novel Inhibitors of Cytokine-induced I $\kappa$ B $\alpha$  Phosphorylation and Endothelial Cell Adhesion Molecule Expression Show Anti-inflammatory Effects in Vivo. *J Biol Chem* 272:21096–21103.
20. Mori N, et al. (2002) Bay 11-7082 inhibits transcription factor NF- $\kappa$ B and induces apoptosis of HTLV-I-infected T-cell lines and primary adult T-cell leukemia cells. *Blood* 100:1828–1834.
21. Loughran TP, Jr., Aprile JA, Ruscetti FW (1990) Anti-CD3 monoclonal antibody-mediated cytotoxicity occurs through an interleukin-2-independent pathway in CD3+ large granular lymphocytes. *Blood* 75:935–940.
22. Kothapalli R, et al. (2003) Constitutive expression of cytotoxic proteases and down-regulation of protease inhibitors in LGL leukemia. *Int J Oncol* 22:33–39.
23. Yang J, et al. (2008) Antigen activation and impaired Fas-induced death-inducing signaling complex formation in T-large-granular lymphocyte leukemia. *Blood* 111:1610–1616.
24. Liu K, Catalfamo M, Li Y, Henkart PA, Weng N-p (2002) IL-15 mimics T cell receptor crosslinking in the induction of cellular proliferation, gene expression, and cytotoxicity in CD8+ memory T cells. *Proc Natl Acad Sci USA* 99:6192–6197.
25. Weng N-P, Liu K, Catalfamo M, Li YU, Henkart PA (2002) IL-15 is a growth factor and an activator of CD8 memory T cells. *Ann NY Acad Sci* 975:46–56.
26. Fehniger TA, et al. (2001) Fatal leukemia in interleukin 15 transgenic mice follows early expansions in natural killer and memory phenotype CD8+ T cells. *J Exp Med* 193:219–232.
27. Hsu C, et al. (2007) Cytokine-independent growth and clonal expansion of a primary human CD8+ T-cell clone following retroviral transduction with the IL-15 gene. *Blood* 109:5168–5177.
28. Mannaioni PF, Di Bello MG, Masini E (1997) Platelets and inflammation: Role of platelet-derived growth factor, adhesion molecules and histamine. *Inflammation Res* 46:4–18.
29. Daynes RA, Dowell T, Araneo BA (1991) Platelet-derived growth factor is a potent biologic response modifier of T cells. *J Exp Med* 174:1323–1333.
30. Hayden MS, West AP, Ghosh S (2006) NF- $\kappa$ B and the immune response. *Oncogene* 25:6758–6780.
31. Intlekofer AM, et al. (2005) Effector and memory CD8+ T cell fate coupled by T-bet and eomesodermin. *Nat Immunol* 6:1236–1244.
32. Hamann D, et al. (1997) Phenotypic and functional separation of memory and effector human CD8+ T cells. *J Exp Med* 186:1407–1418.
33. Nath N, Prasad R, Giri S, Singh AK, Singh I (2006) T-bet is essential for the progression of experimental autoimmune encephalomyelitis. *Immunology* 118:384–391.
34. Solomou EE, Keyvanfar K, Young NS (2006) T-bet, a Th1 transcription factor, is up-regulated in T cells from patients with aplastic anemia. *Blood* 107:3983–3991.
35. Juedes AE, Rodrigo E, Togher L, Glimcher LH, von Herrath MG (2004) T-bet controls autoaggressive CD8 lymphocyte responses in type 1 diabetes. *J Exp Med* 199:1153–1162.
36. Lovett-Racke AE, et al. (2004) Silencing T-bet defines a critical role in the differentiation of autoreactive T lymphocytes. *Immunity* 21:719–731.
37. Albert R, et al. (2007) A novel method for signal transduction network inference from indirect experimental evidence. *J Comput Biol* 14:927–949.
38. Kachalo S, Zhang R, Sontag E, Albert R, DasGupta B (2008) NET-SYNTHESIS: A software for synthesis, inference and simplification of signal transduction networks. *Bioinformatics* 24:293–295.